

Unconventional Translation of C9ORF72 **GGGGCC Expansion Generates Insoluble** Polypeptides Specific to c9FTD/ALS

Peter E.A. Ash,^{1,3,4} Kevin F. Bieniek,^{1,3,4} Tania F. Gendron,¹ Thomas Caulfield,¹ Wen-Lang Lin,¹ Mariely DeJesus-Hernandez, 1,3 Marka M. van Blitterswijk, 1 Karen Jansen-West, 1 Joseph W. Paul III, 1 Rosa Rademakers, 1 Kevin B. Boylan,² Dennis W. Dickson,¹ and Leonard Petrucelli^{1,*}

http://dx.doi.org/10.1016/j.neuron.2013.02.004

SUMMARY

Frontotemporal dementia (FTD) and amyotrophic lateral sclerosis (ALS) are devastating neurodegenerative disorders with clinical, genetic, and neuropathological overlap. Hexanucleotide (GGGGCC) repeat expansions in a noncoding region of C9ORF72 are the major genetic cause of FTD and ALS (c9FTD/ALS). The RNA structure of GGGGCC repeats renders these transcripts susceptible to an unconventional mechanism of translation—repeatassociated non-ATG (RAN) translation. Antibodies generated against putative GGGGCC repeat RANtranslated peptides (anti-C9RANT) detected high molecular weight, insoluble material in brain homogenates, and neuronal inclusions throughout the CNS of c9FTD/ALS cases. C9RANT immunoreactivity was not found in other neurodegenerative diseases, including CAG repeat disorders, or in peripheral tissues of c9FTD/ALS. The specificity of C9RANT for c9FTD/ALS is a potential biomarker for this most common cause of FTD and ALS. These findings have significant implications for treatment strategies directed at RAN-translated peptides and their aggregation and the RNA structures necessary for their production.

INTRODUCTION

Frontotemporal dementia (FTD) and amyotrophic lateral sclerosis (ALS) are devastating diseases with no effective treatment. FTD, a common cause of early-onset dementia, encompasses a group of disorders distinguished clinically by abnormalities in behavior, language, and personality, while ALS is characterized by the degeneration of motor neurons, leading to muscle atrophy and paralysis. Because of significant clinical and neuropathological overlap, FTD and ALS are thought to represent a disease spectrum (Van Langenhove et al., 2012). Frontal lobe impairment is increasingly recognized in ALS (Phukan et al., 2012) and a subset of FTD patients develops features of motor neuron disease. Furthermore, most ALS cases and the most common pathological subtype of FTD (FTLD-TDP) are associated with neuronal and glial TDP-43-positive inclusions (Neumann et al., 2006). Two independent groups recently identified a hexanucleotide (GGGGCC) repeat expansion in a noncoding region of C9ORF72 as the most frequent genetic cause of ALS and FTD (c9FTD/ALS) (DeJesus-Hernandez et al., 2011; Renton et al., 2011), firmly establishing a genetic link between the two disorders. In addition to TDP-43 inclusions, a characteristic finding of c9FTD/ALS is the presence of TDP-43-negative, p62/sequestosome-1-positive neuronal inclusions in the cerebellum and hippocampus (Al-Sarraj et al., 2011; Pikkarainen et al., 2010). These inclusions are also immunoreactive for ubiquitin and select ubiquitin-binding proteins, most notably ubiquilin-2 (Bieniek et al., 2013; Brettschneider et al., 2012).

While the mechanisms of disease of c9FTD/ALS remain unknown, several groups have shown that mRNA levels of at least one C9ORF72 transcript are decreased in c9FTD/ALS (DeJesus-Hernandez et al., 2011; Gijselinck et al., 2012; Renton et al., 2011), suggesting a potential loss of function. While the normal function of the C9ORF72 protein remains obscure, it is structurally related to DENN domain proteins, highly conserved GDP-GTP exchange factors for Rab GTPases (Levine et al., 2013; Zhang et al., 2012). The accumulation of RNA transcripts containing the GGGCC repeat within nuclear foci in frontal cortex and spinal cord in c9FTD/ALS also suggests a toxic RNA gain of function (DeJesus-Hernandez et al., 2011). RNA foci, which lead to the sequestration and altered activity of RNA-binding proteins, have been implicated in several noncoding expansion disorders (Renoux and Todd, 2012). Another possible pathogenic mechanism is repeat associated non-ATG translation (RAN translation). RAN translation, an unconventional mode of translation that occurs in the absence of an initiating ATG codon, was first described by Ranum and coworkers (Zu et al., 2011), who reported that RAN translation across expanded CAG repeats occurs in all reading frames (CAG, AGC, and GCA) to produce homopolymeric proteins of long



¹Department of Neuroscience

²Department of Neurology

Mayo Clinic Florida, Jacksonville, FL 32224, USA

Mayo Graduate School, Mayo Clinic College of Medicine, Rochester, MN 55905, USA

⁴These authors contributed equally to this work

^{*}Correspondence: petrucelli.leonard@mayo.edu



polyglutamine, polyserine, or polyalanine tracts. Of particular importance, polyalanine and polyglutamine proteins, respectively, were found to accumulate in disease-relevant tissues of patients with spinocerebellar ataxia type 8 and myotonic dystrophy type 1 (Zu et al., 2011).

Given that canonical rules of translation may not apply in disorders associated with repeat expansions, we sought to determine whether RAN translation products of expanded GGGGCC are produced in c9FTD/ALS. Three two-amino acid alternating copolymers—(glycine-alanine)_n, (glycine-arginine)_n, and (glycine-proline)_n—could theoretically be expressed by RAN translation of the sense transcript of the expanded GGGGCC repeat in *C9ORF72*. To explore this possibility, we generated polyclonal antibodies with high specificity and sensitivity to putative RAN translation products and have identified a novel neuropathology specific to c9FTD/ALS.

RESULTS

The detection of nuclear foci containing RNA transcripts containing the expanded GGGCC repeat in cortical and spinal cord neurons of c9FTD/ALS cases (DeJesus-Hernandez et al., 2011) indicates that these transcripts are expressed and thus possibly available for RAN translation. Given evidence that RAN translation of expanded CAG repeats depends on hairpin formation (Zu et al., 2011), we sought to determine the structure of expanded GGGCC repeats using the latest methodologies for generating secondary structure predictions (SSPs) (Gardner et al., 2011). Shown in Figure S1A, available online, is the major RNA SSP for ten GGGGCC repeats (60 bases). For comparison, the SSP for 20 repeats (60 bases) of the CAG trinucleotide is shown. Note that both structures form stable hairpins, with the GGGGCC repeat structure having a lower composite global energy ($\Delta G = -40.80$ kcal/mol), and thus greater stability, than CAG repeats of equal length ($\Delta G = -19.60$). In fact, GGGGCC repeats become successively more stable as repeat length increases, having a ∆G of −242.80 and −1,000.30 kcal/mol for repeats of 300 and 1,200 bases, respectively. Given these observations, the GGGCC repeat may be subject to RAN translation.

To elucidate whether RAN translation products are indeed expressed in c9FTD/ALS, we generated two independent polyclonal antibodies (termed anti-C9RANT) by immunizing two rabbits using the pooled synthetic peptides (GA)₈, (GP)₈, and (GR)₈ as antigens. These peptides were chosen because RAN translation of (GGGGCC)_n transcripts in the three alternate reading frames would produce poly-(glycine-alanine), poly-(glycine-proline), and poly-(glycine-arginine) peptides (Figure 1A).

To determine selectivity of both C9RANT antibodies to glycine-alanine, glycine-proline, and glycine-arginine tracts, we performed quantitative indirect immunoassays using Meso Scale Discovery (MSD) electrochemiluminescence detection technology. Measurement of anti-C9RANT binding to immobilized (GA)₈, (GP)₈, or (GR)₈ peptides shows that both anti-C9RANT antibodies bound the (GP)₈ peptide in a dosedependent manner, with relatively little binding to (GA)₈ and (GR)₈ and no binding to the negative control peptides (GK)₈ and (GX)₈ (Figures 1B and 1C). Consistent with these findings, anti-C9RANT selectively detected exogenously expressed

GFP-tagged (GP) $_5$ in HeLa cell lysates, as assessed by western blot (Figure S1B). Immunofluorescence staining of HeLa cells transfected to express the various GFP-tagged peptides also showed that (GP) $_5$ was immunoreactive for anti-C9RANT, but not (GA) $_5$ or (GR) $_5$ or the negative controls (GK) $_5$ and (GX) $_5$ (Figure S1C). GFP-tagged (GP) $_5$, (GR) $_5$, and (GA) $_5$ were expressed in the cytoplasm and nucleus of cells. Of note, (GP) $_5$ and (GR) $_5$ assembled into punctate structures in the cytoplasm, whereas (GA) $_5$ expression remained diffuse. These results show the generation of two C9RANT polyclonal antibodies that preferentially detect poly-(glycine-proline) peptides.

To evaluate whether RAN translation products are expressed in c9FTD/ALS, we performed western blot analysis of urea fractions from cerebellar tissue of FTLD and ALS cases with or without expanded GGGCC repeats. Cerebellar tissue was utilized in view of the cerebellar pathology observed in c9FTD/ ALS. Notably, insoluble anti-C9RANT-immunoreactive high molecular weight material was observed only in samples from C9ORF72 mutation carriers (Figure 1D, arrow). Due to the large size of these products, they became trapped at the top of the stacking gel. To overcome this issue, we conducted dot blots using the cerebellar urea fractions. Anti-C9RANT-immunoreactivity was specific to c9FTD/ALS and was not detected in cases lacking pathogenic repeat expansions in C9ORF72 (Figure 1E and Figure S1D). Consistent with these findings, immunohistochemical analysis revealed that anti-C9RANT-immunoreactive neuronal cytoplasmic inclusions were abundant in the cerebellum of c9FTD/ALS cases (Figures 1F and 1H) but absent in FTLD-TDP cases with no C9ORF72 repeat expansion (Figures 1G and 1I). Note that the C9RANT antibodies generated from two independent rabbits showed similar staining profiles. For consistency, subsequent immunohistochemical studies were conducted using the antibody (Rb5823) with the least background.

The above results indicate that poly-(glycine-proline) peptides are specifically expressed in c9FTD/ALS. To evaluate whether their production results from the translation of expanded GGGGCC repeats in the absence of an ATG-initiating codon, we sequenced DNase1-treated pre-mRNA collected from cerebellar tissue of two c9FTD and two control cases. Sequences obtained matched the previously reported *C9ORF72* genomic sequence (AL451123.12). The ATG nearest to the GGGGCC repeat was observed 247 base pairs upstream; however, multiple stop codons within each frame are present in the 240 base pairs upstream of the repeat, thus placing stop codons between the ATG and the expanded repeat.

Next, the regional distribution of C9RANT immunoreactivity within the CNS of c9FTD/ALS cases was assessed by immuno-histochemistry, revealing widespread neuronal cytoplasmic and intranuclear inclusions (Figure 2). The inclusions were morphologically similar to TDP-43-negative inclusions noted in previous studies with ubiquitin or ubiquitin binding (p62 and ubiquilin-2) immunohistochemistry (Al-Sarraj et al., 2011; Bigio et al., 2012). C9RANT-immunoreactive inclusions were exclusively found in gray matter and within neurons. They were not detected in vascular endothelial or smooth muscle cells or in white matter or glia. Nonetheless, given the growing recognition of intercellular communication in neurodegeneration (Garden and La



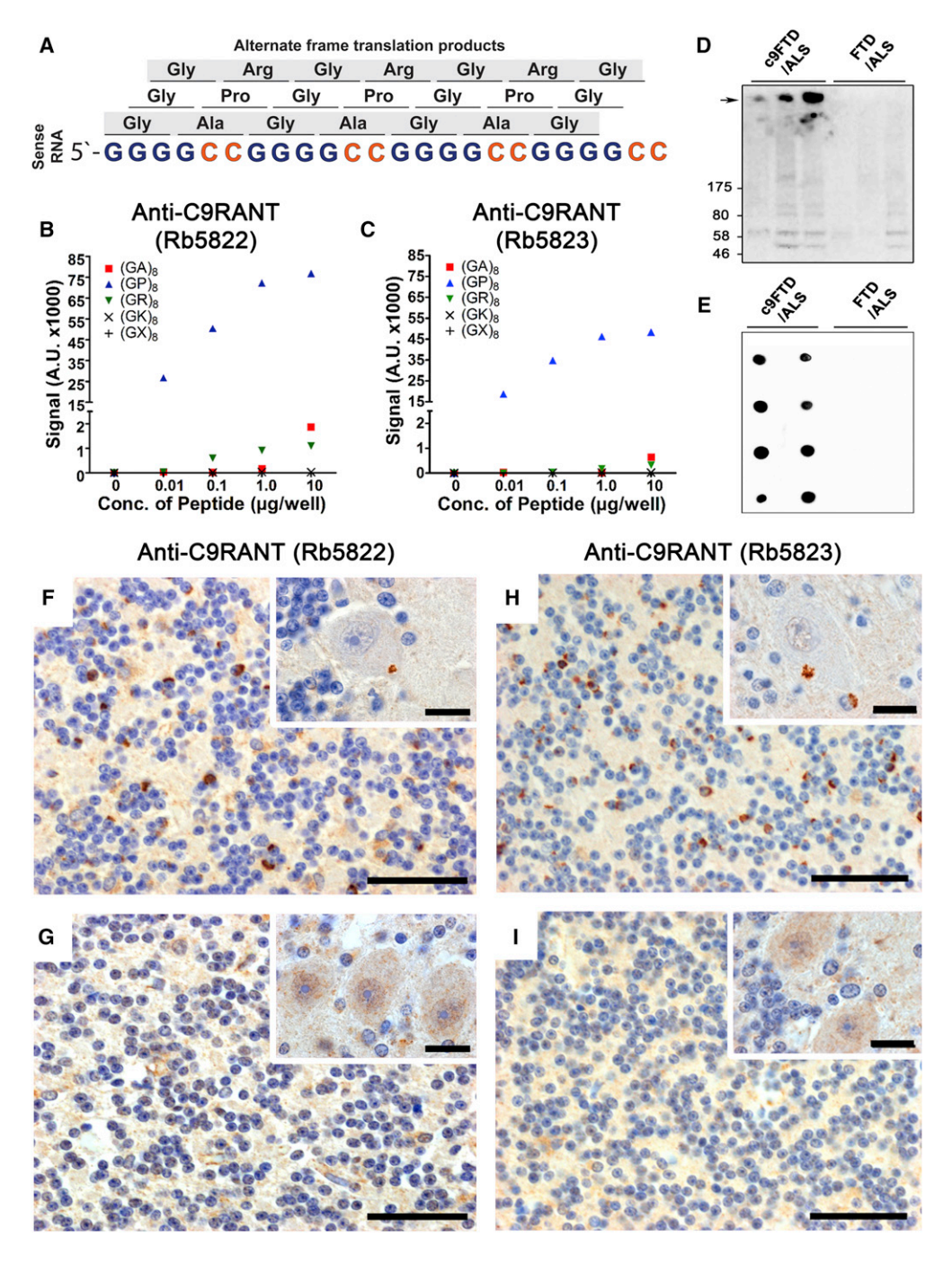
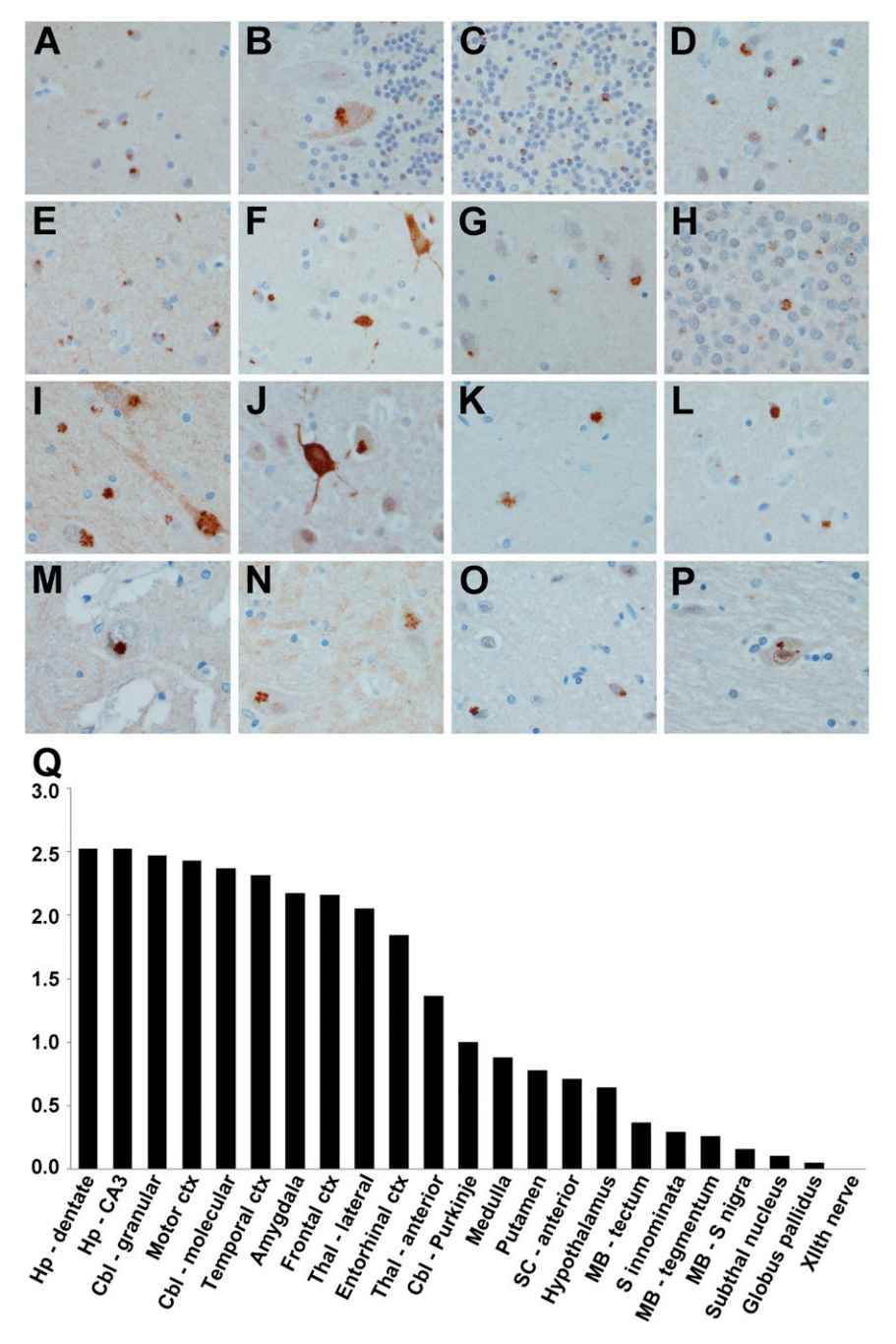


Figure 1. Anti-C9RANT Immunoreactivity Is Specific to c9FTD/ALS

(A) Schematic representation of the possible protein products generated by RAN translation of expanded GGGGCC repeats in the three alternate reading frames. (B and C) Immunoreactivity of each anti-C9RANT antibody (Rb5822 and Rb5823) toward indicated peptides was measured by adsorbing peptides onto carbon electrodes in 96-well MSD plates and coincubating wells with anti-C9RANT and a SULFO-tagged anti-rabbit secondary antibody. Anti-C9RANT binding to respective peptides was quantified by measuring the intensity of emitted light upon electrochemical stimulation of the plate using the MSD Sector Imager 2400. The amino acid sequence for (GX)₅ is Gly-Met-Gly-Ser-Gly-Leu-Gly-Thr. (D) Western blot analysis of cerebellar tissue urea fractions from C9ORF72 repeat expansion and nonexpansion FTLD cases using anti-C9RANT. Note the high molecular weight product (arrow). (E) Anti-C9RANT immunoreactivity in cerebellar urea fractions from FTLD-TDP and ALS cases with or without expanded GGGGCC repeats, as assessed by dot blot. Each dot represents one case. See also Figure S1. (F-I) Immunohistochemistry with each anti-C9RANT antibody revealed that abundant neuronal inclusion in the cerebellum of c9FTD (F and H), but not in sporadic FTLD-TDP (G and I). C9RANT-immunoreactive lesions were granular neuronal cytoplasmic inclusions (seen clearly in the Purkinje cell shown in insets in F and H). Scale bar represents 50 μm in main images and 20 μm in insets.





Spada, 2012), the neuronal localization of C9RANT inclusions was validated by double-labeled immunofluorescence analysis of c9FTD hippocampal tissue (Figure 3). The granular cytoplasmic and intranuclear inclusions were found in neuronal populations immunopositive for microtubule-associated protein 2 (MAP2) but not in astrocytes immunopositive for glial fibrillary acidic protein (GFAP).

Neuronal cytoplasmic inclusions immunoreactive for anti-C9RANT were coarsely granular and sometimes "star shaped" (Figure 2). In contrast, neuronal intranuclear inclusions were small round lesions (Figure 4A). C9RANT-immunoreactive inclu-

Figure 2. Regional Neuropathology **C9RANT**

(A-P) C9BANT-immunoreactive neuronal inclusions were observed throughout the CNS, including cerebellum (A, cerebellar molecular layer; B, cerebellar Purkinie cell laver: C. cerebellar internal granular layer), neocortex (D, frontal cortex; E, temporal cortex; F, motor cortex), subcortical gray matter (G, amygdala; H, dentate gyrus of the hippocampus; I, CA3 of the hippocampus; J, lateral geniculate nucleus: K. lateral thalamus: L. medial geniculate nucleus; N, globus pallidus; O, hypothalamus: P. nucleus basalis of Mevnert), and to a lesser extent the brainstem (M. substantia nigra). (Q) Semiquantitative pathology scoring in these aforementioned regions and in the entorhinal cortex, medulla, putamen, midbrain, and spinal cord reveals variable C9RANT-immunoreactive inclusions throughout the CNS. Cbl, cerebellum; ctx, cortex; Hp, hippocampus; MB, midbrain; S, substantia; SC, spinal cord; Subthal, subthalamic; Thal, thalamus.

sions were frequent in granular neurons (e.g., dentate gyrus of hippocampus and internal granular cell layer of cerebellum; Figures 2C and 2H) but were also detected in large neurons (e.g., pyramidal neurons in the neocortex and cerebellar Purkinje cells; Figures 2B and 2l). The frequency of C9RANT-immunoreactive neuronal inclusions in any given region was variable. To gain an understanding of the distribution, we scored the density of lesions in 24 brain regions of 30 cases of c9FTD/ALS (Figure 2Q). Inclusions were detected in most abundance in regions previously shown to be affected in c9FTD/ALS with p62 immunohistochemistry, including the neocortex, hippocampus, and cerebellum (Pikkarainen et al., 2008, 2010), but they were also present in regions not previously considered to be affected, such as medial and lateral geniculate nuclei (Figure 2Q). The lesion burden tended to be greater in limbic structures (e.g., hippocampus

and amygdala) and neocortex than in subcortical gray matter and brainstem, but the most severely affected region in most cases was the cerebellar cortex.

To further determine specificity of C9RANT immunoreactivity for c9FTD/ALS, we performed immunohistochemistry on hippocampus and cerebellum of 44 FTLD-TDP and 6 ALS cases lacking the C9ORF72 repeat expansion, as well as 65 cases with other neurodegenerative diseases (Alzheimer's disease, diffuse Lewy body disease [some of which presented clinically as Parkinson's disease and demential, multiple system atrophy, progressive supranuclear palsy, and corticobasal degeneration)



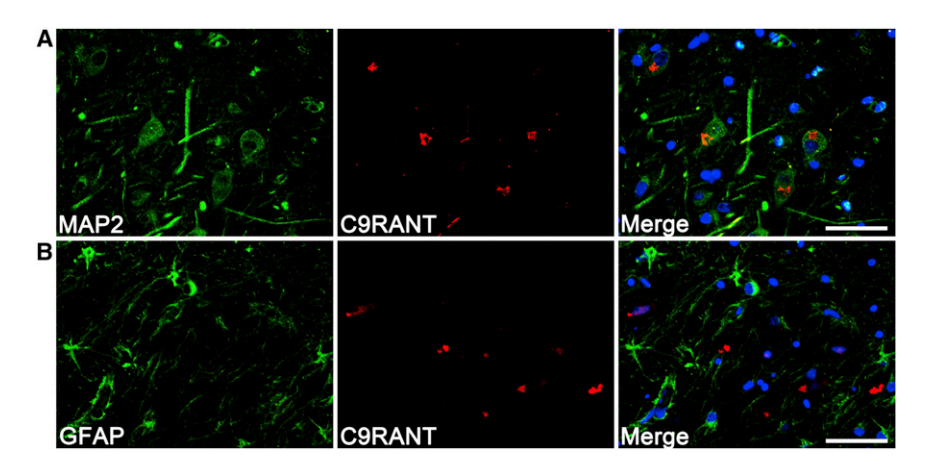


(Table S1). In none of these cases did we detect C9RANT-immunoreactive lesions (Figure S2). Given that RAN translation is reported in other repeat disorders (Zu et al., 2011), we also performed immunohistochemistry on vulnerable brain regions in Huntington disease (basal ganglia), spinocerebellar ataxia type 3 (pons), and Kennedy's spinal and bulbar muscular atrophy (medulla). All cases had characteristic neuronal intranuclear inclusions with p62 immunohistochemistry, but none had C9RANT-immunoreactive neuronal inclusions in either nucleus or cytoplasm (Figures 4A-4H).

Given the specificity of anti-C9RANT for neuronal inclusions throughout the CNS of c9FTD/ALS, it was of interest to know whether lesions would be detected in peripheral tissues. Sections from skeletal muscle, peripheral nerve, dorsal root ganglia, heart, lung, liver, spleen, kidney, and testes were processed for C9RANT immunohistochemistry from three c9FTD/ ALS cases and a sporadic FTLD-TDP case (Figures 4I-4L). No C9RANT-immunoreactive inclusions were detected in other organs, including peripheral nerves and ganglia. The only exception was the testes, where C9RANT immunoreactivity was detected in both cytoplasmic and nuclear inclusions in Sertoli cells, but not in germ cells of the seminiferous tubules (Figure 4L) in the c9FTD/ALS cases and not the FTLD-TDP

DISCUSSION

The discovery of a neuropathology specific to c9FTD/ALS, namely the accumulation of poly-(glycine-proline) peptides, provides insight into the pathobiology of c9FTD/ALS. While it remains to be determined whether polypeptides generated by RAN translation are neurotoxic, the findings herein expand the possible mechanisms of disease in c9FTD/ALS. Our findings show C9RANT-immunoreactive lesions in both neuronal populations that are generally not affected in neurodegenerative disease processes (e.g., neurons of lateral geniculate nucleus), as well as in vulnerable areas (e.g., neurons of neocortex and hippocampus).

The initiation of RAN translation is thought to depend on RNA hairpin structures that utilize C:G complementary pairing. Long tracts of CAG repeats that form hairpins and multibranched structures undergo RAN translation, whereas CAA repeats of

Figure 3. C9RANT-Immunoreactive Inclusions Are Present in Neurons but Not **Astrocytes**

Double-label immunofluorescence was performed on hippocampal tissue from a c9FTD case using anti-C9RANT (Rb5823) antiserum and the neuronal marker MAP2 or the astrocytic marker GFAP. Note that C9RANT-immunoreactive inclusions localize exclusively to neurons (A) and are not found in astrocytes (B). Scale bar represents 50 µm.

similar length do not form hairpins and are not RAN translated (Zu et al., 2011). Using established methods for predicting the RNA secondary structure of

GGGCC repeats, we found that an imperfect doublestranded-like conformation is energetically preferred, similar to our prediction models for CAG repeat RNA and to CAG repeat structures previously derived by alternative methods (de Mezer et al., 2011). GGGGCC RNA transcripts are therefore likely to form stable hairpins and, consequently, may undergo RAN translation. Nonetheless, it must be noted that the precise RNA structural features involved in RAN translation initiation remain to be fully elucidated.

To determine whether there is evidence of RAN translation in c9FTD/ALS, we immunized two rabbits with pooled (GA)₈, (GP)₈, and (GR)₈ peptides. Using a variety of approaches, we show that both C9RANT antibodies preferentially detect poly-(glycine-proline), having little or no immunoreactivity toward poly-(glycine-arginine) or poly-(glycine-alanine), depending on the assay employed. Of importance, anti-C9RANT antibodies had disease specificity, showing binding to neuronal inclusions in c9FTD/ALS, but not to neuronal or glial inclusions in a range of other common neurodegenerative diseases or to intranuclear inclusions in several CAG trinucleotide repeat disorders. Additional screening of other repeat disorders would be important, since the number of cases of trinucleotide repeat disorders screened for C9RANT-immunoreactive pathology was small. The biochemical correlate of C9RANT-positive inclusions was high molecular weight and insoluble material comparable to that present in other disorders with insoluble neuronal inclusions, most notably tau in Alzheimer's disease. This insoluble material was present in homogenates from brain regions with dense C9RANT-immunoreactive pathology, in particular the cerebellum, of c9FTD/ALS cases, but not in ALS or FTLD cases negative for the C9ORF72 expanded repeat.

C9RANT immunoreactivity was, with the exception of testes, specific to the CNS, despite the fact that wild-type C9ORF72 transcripts are expressed in peripheral tissues (DeJesus-Hernandez et al., 2011). It is interesting to note that the semiquantitative PCRs suggest that expression levels of GGGGCCcontaining transcript are highest in the brain and testes, the same regions where C9RANT immunoreactivity is observed. Conversely, the short transcript variant, which is not predicted to contain the GGGGCC sequence, is expressed equally in CNS and peripheral tissues.



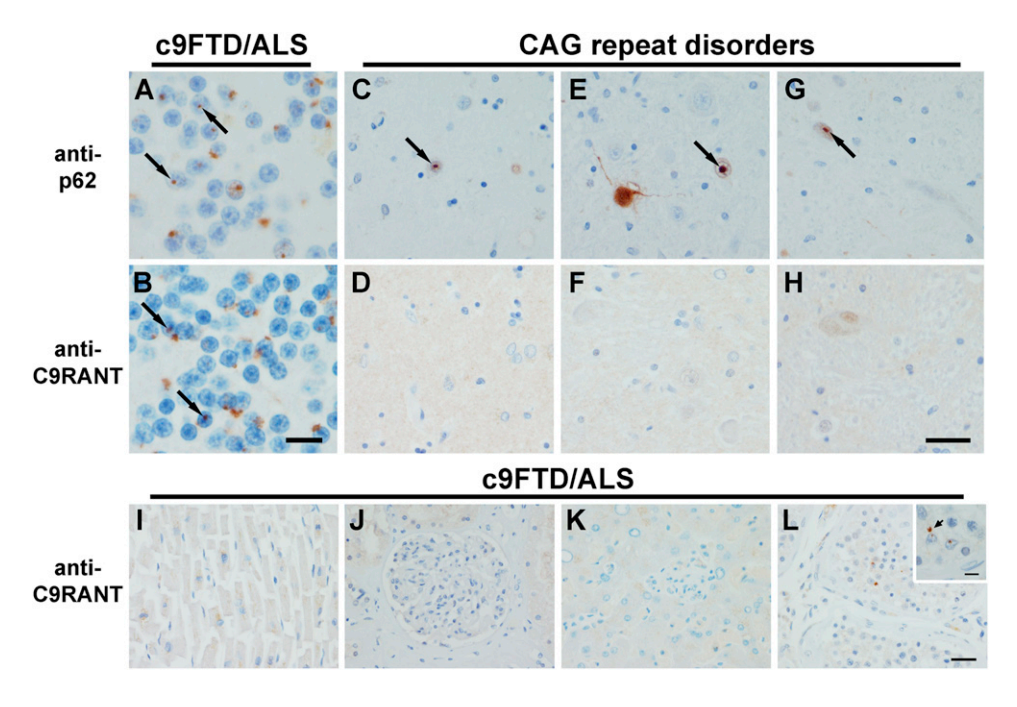


Figure 4. Specificity of C9RANT Pathology

p62 immunolabeling of neuronal intranuclear inclusions (arrows) in c9FTD/ALS (A, cerebellum), Huntington disease (C, basal ganglia), spinocerebellar ataxia type 3 (E, pons), and spinal and bulbar muscular atrophy (Kennedy's disease) (G, medulla). Anti-C9RANT-positive inclusions are specific to c9FTD/ALS (B) and absent from these other CAG repeat disorders (D, Huntington disease; F, spinocerebellar ataxia type 2; H, Kennedy's disease). Additionally, C9RANT pathology is predominantly neuronal, with no inclusions in the heart (I), kidney (J), or spleen (K). The only other organ where C9RANT lesions were found was the testes, where C9RANT-immunoreactive cytoplasmic and nuclear inclusions were noted in Sertoli cells (L). Scale bars in (H) and (L) represent 30 μm; scale bars in (B) and inset of (L) represent 6 μm. See also Figure S2 and Table S1.

The specificity of anti-C9RANT immunoreactivity serves as an encouraging step in the development of a biomarker for c9FTD/ALS. Although the repeat-primed PCR method to screen for c9FTD/ALS is fast and cost effective, GGGGCC repeat size determined using DNA from whole blood may not accurately reflect repeat size in the brain or spinal cord due to somatic heterogeneity and varying repeat sizes in different tissues from a single patient (van Blitterswijk et al., 2012). The development of anti-C9RANT immunoassays is warranted to investigate C9RANT immunoreactivity in cerebrospinal fluid as a potential marker of disease activity and/or progression.

We provide clear evidence that the accumulation of poly-(glycine-proline) peptides is a pathognomonic feature of c9FTD/ALS. These results do not, however, rule out the possible accumulation of other translated products from the expanded GGGCC repeat. As mentioned, the alternate frames of sense GGGGCC RNA may be translated, producing poly-(glycinealanine) and poly-(glycine-arginine) peptides. While we cannot exclude the possibility of ATG-initiated translation of GGGGCC repeat-containing transcripts, poly-(glycine-proline) peptides probably result from unconventional translation of the GGGGCC expansion located in an intronic region of C9ORF72, given that STOP codons occur in each of the translation frames of the sense transcript upstream of the repeat. It is also worth noting that antisense RNA is generated in several repeat disorders (Renoux and Todd, 2012), and if this phenomenon is reproduced with the C9ORF72 hexanucleotide expansion, RAN translation of CCCCGG antisense RNA could result in the production of poly-(proline-alanine), poly-(proline-glycine), and poly-(proline-arginine). Further work is required to discover the existence of the antisense transcript and the origin of translation initiation.

Given that the abnormal accumulation of insoluble proteins has been associated with neuronal dysfunction and degeneration in many neurodegenerative diseases, the identification of disease-specific C9RANT-positive pathology in patients with a C9ORF72 repeat expansion may offer valuable insight on disease mechanism and potential therapeutic strategies. Not only may the abnormal aggregation of RAN translation products be targeted, but so too could the formation of RNA structures thought critical for RAN translation.

EXPERIMENTAL PROCEDURES

Structure Prediction of GGGGCC Sequences

The SSP for GGGGCC and CAG repeats was modeled using RNA prediction packages MFOLD, Sfold, and Vienna RNA Package (RNAfold). Details are provided in the Supplemental Experimental Procedures.

Generation of C9RANT Antibodies

Each of two rabbits (Rb5822 and Rb5823) was immunized with the following three pooled peptides: C-Ahx-(GA)₈-amide, C-Ahx-(GP)₈-amide, and C-Ahx-(GR)₈-amide. Preimmune serum from each rabbit was tested against peptide antigens and tissue from c9FTD/ALS cases by immunohistochemistry and confirmed negative. Antiserum was used directly or purified with Protein A or G affinity columns.



Meso Scale Discovery Immunoassays

Quantitative indirect immunoassays using anti-C9RANT antibodies were performed using the Meso Scale Discovery (MSD) electrochemiluminescence platform, as described in the Supplemental Experimental Procedures.

Sequential Fractionation and Analysis of Frozen Cerebellar Tissue

Tissues utilized for all experiments within this study were obtained from cases negative or positive for expanded repeats in C9ORF72, as determined by a two-step protocol (DeJesus-Hernandez et al., 2011). Protein was sequentially extracted from frozen cerebellar tissue as previously described by Neumann et al. (2006). Urea fractions were mixed, but not boiled, in SDS sample buffer containing 5% $\beta\text{-mercaptoethanol}$ and run on 10% Tris-Glycine Novex gels (Invitrogen). Samples were transferred to PVDF membranes, blocked in 5% nonfat dry milk, and probed with anti-C9RANT. For dot blots, urea fractions (2 µl per sample) were dotted directly to nitrocellulose membrane, which were then blocked and probed with anti-C9RANT. See the Supplemental Experimental Procedures for details.

RNA Sequencing Methods

RNA was collected from frozen cerebellar tissue using QIAGEN RNeasy Plus mini kits with genomic DNA eliminator columns and an additional on column RNase-free DNase1 treatment. RNA was reverse transcribed to cDNA with either oligo dTs or random hexamers (Invitrogen). PCR products were amplified in the pre-mRNA region, upstream of the GGGGCC repeat, using the forward primer 5'- CTACGGTGTCCCGCTAGGAAAG and the reverse primer 5'- GGCCCCTAGCGCGCGACTCCTGAG and downstream of the repeat using the forward primer 5'- GGGGCGTGGTCGGGGCCCGG and the reverse primer 5'- AAGGAGACAGCTCGGGTACTGA. The junction of noncodon exon 1a to exon 2 in mature transcript variants 1 (NM 145005.5) and 3 (NM_001256054.1) was amplified with the forward primer 5'- AAAGATGA CGCTTGGTGTC and the reverse primer 5'- TATGAAGTGGGAGGTAGA AAC. Sequencing of amplicons was performed with the same primers using Big Dye Terminator v3.1 (Applied Biosciences), cleaned by Montage vacuum plates (Millipore), analyzed on an ABI3730 (Applied Biosciences), and viewed with Sequencher software (Gene Codes).

Immunohistochemistry of Central and Peripheral Nervous System

Anti-C9RANT (Rb5823) immunoreactivity was examined in postmortem tissue from 21 FTLD and 9 ALS C9ORF72 mutation carriers. Sections from the frontal and temporal cerebral cortices, hippocampus, cerebellum, basal ganglia, amygdala, thalamus, midbrain, and spinal cord (if available) were stained with C9RANT antiserum (1:5,000). In three C9ORF72-linked FTD/ALS cases, anti-C9RANT pathology from multiple tissue types was examined, including heart, lung, spleen, liver, kidney, muscle, peripheral nerve, and testis. The hippocampus or basal forebrain was also studied in 123 control cases, including 41 sporadic FTLD, 6 sporadic ALS (1 was matched control for the other organs), 3 FTLD cases due to GRN mutation, 15 Alzheimer's disease, 15 multiple system atrophy, 15 diffuse Lewy body disease, 14 progressive supranuclear palsy, 6 corticobasal degeneration disease, 2 Huntington disease, 1 spinocerebellar ataxia type 3, 1 spinal and bubal muscular atrophy (Kennedy's disease), 1 dentato-rubro-pallido-luysian atrophy, and 3 cognitively normal cases. Cases were stained with anti-C9RANT or mouse monoclonal p62 (BD Biosciences) using previously published methods (Bieniek et al., 2013). Deidentified postmortem brain samples used in this study have been deemed "exempt" as defined by federal regulations for human subject research. All autopsies were obtained after informed consent of the legal next of kin, and brain banking procedures conform to ethical guidelines of the Mayo Clinic Institutional Review Board (IRB). See the Supplemental Experimental Procedures for details.

Double-Label Immunofluorescence

Double-label immunofluorescence was performed on hippocampal tissue from a c9FTD case using anti-C9RANT (Rb5823) antiserum and cell typespecific antibodies. See the Supplemental Experimental Procedures for details.

SUPPLEMENTAL INFORMATION

Supplemental Information includes two figures, one table, and Supplemental Experimental Procedures and can be found with this article online at http:// dx.doi.org/10.1016/j.neuron.2013.02.004.

ACKNOWLEDGMENTS

We are grateful to all patients, family members, and caregivers who agreed to brain donation, without which these studies would have been impossible. We also acknowledge expert technical assistance of Linda Rousseau, Virginia Phillips, and Monica Castanedes-Casey for histology and John Gonzalez, Beth Marten, Pamela Desaro, and Amelia Johnston for brain banking. This work was supported by Mayo Clinic Foundation, National Institutes of Health/ National Institute on Aging (R01 AG026251 [L.P., R.R.], P01 AG003949 [D.W.D.], P50 AG016574 [D.W.D., R.R.]), National Institutes of Health/National Institute of Neurological Disorders and Stroke (R21 NS074121-01 [T.F.G., K.B.B.], R01 NS080882 [R.R.], R01 NS063964 [L.P.], R01 NS077402 [L.P.], P50 NS72187 [D.W.D., R.R.]), National Institute of Environmental Health Services (R01 ES20395 [L.P.]), Amyotrophic Lateral Sclerosis Association (K.B.B., L.P.), ALS Therapy Alliance (R.R.), and Department of Defense (W81XWH-10-1-0512-1 [L.P.], W81XWH-09-1-0315AL093108 [L.P.]). R.R. and M.D.-H. have a patent on the discovery of the hexanucleotide repeat expansion in the C9ORF72 gene.

Accepted: February 4, 2013 Published: February 12, 2013

REFERENCES

Al-Sarraj, S., King, A., Troakes, C., Smith, B., Maekawa, S., Bodi, I., Rogelj, B., Al-Chalabi, A., Hortobágyi, T., and Shaw, C.E. (2011). p62 positive, TDP-43 negative, neuronal cytoplasmic and intranuclear inclusions in the cerebellum and hippocampus define the pathology of C9orf72-linked FTLD and MND/ ALS. Acta Neuropathol. 122, 691-702.

Bieniek, K.F., Murray, M.E., Rutherford, N.J., Castanedes-Casey, M., Dejesus-Hernandez, M., Liesinger, A.M., Baker, M.C., Boylan, K.B., Rademakers, R., and Dickson, D.W. (2013). Tau pathology in frontotemporal lobar degeneration with C9ORF72 hexanucleotide repeat expansion. Acta Neuropathol. 125, 289-302.

Bigio, E.H., Weintraub, S., Rademakers, R., Baker, M., Ahmadian, S.S., Rademaker, A., Weitner, B.B., Mao, Q., Lee, K.H., Mishra, M., et al. (2012). Frontotemporal lobar degeneration with TDP-43 proteinopathy and chromosome 9p repeat expansion in C9ORF72: clinicopathologic correlation. Neuropathology. Published online June 18, 2012. http://dx.doi.org/10.1111/ j.1440-1789.2012.01332.x.

Brettschneider, J., Van Deerlin, V.M., Robinson, J.L., Kwong, L., Lee, E.B., Ali, Y.O., Safren, N., Monteiro, M.J., Toledo, J.B., Elman, L., et al. (2012). Pattern of ubiquilin pathology in ALS and FTLD indicates presence of C9ORF72 hexanucleotide expansion. Acta Neuropathol. 123, 825-839.

de Mezer, M., Wojciechowska, M., Napierala, M., Sobczak, K., and Krzyzosiak, W.J. (2011). Mutant CAG repeats of Huntingtin transcript fold into hairpins, form nuclear foci and are targets for RNA interference. Nucleic Acids Res. 39, 3852-3863.

DeJesus-Hernandez, M., Mackenzie, I.R., Boeve, B.F., Boxer, A.L., Baker, M., Rutherford, N.J., Nicholson, A.M., Finch, N.A., Flynn, H., Adamson, J., et al. (2011). Expanded GGGCC hexanucleotide repeat in noncoding region of C9ORF72 causes chromosome 9p-linked FTD and ALS. Neuron 72, 245-256

Garden, G.A., and La Spada, A.R. (2012). Intercellular (mis)communication in neurodegenerative disease. Neuron 73, 886-901.

Gardner, D.P., Ren, P., Ozer, S., and Gutell, R.R. (2011). Statistical potentials for hairpin and internal loops improve the accuracy of the predicted RNA structure. J. Mol. Biol. 413, 473-483.



Gijselinck, I., Van Langenhove, T., van der Zee, J., Sleegers, K., Philtjens, S., Kleinberger, G., Janssens, J., Bettens, K., Van Cauwenberghe, C., Pereson, S., et al. (2012). A C9orf72 promoter repeat expansion in a Flanders-Belgian cohort with disorders of the frontotemporal lobar degeneration-amyotrophic lateral sclerosis spectrum: a gene identification study. Lancet Neurol. 11, 54-65.

Levine, T.P., Daniels, R.D., Gatta, A.T., Wong, L.H., and Hayes, M.J. (2013). The product of C9orf72, a gene strongly implicated in neurodegeneration, is structurally related to DENN Rab-GEFs. Bioinformatics. Published online January 16, 2013. http://dx.doi.org/10.1093/bioinformatics/bts725.

Neumann, M., Sampathu, D.M., Kwong, L.K., Truax, A.C., Micsenyi, M.C., Chou, T.T., Bruce, J., Schuck, T., Grossman, M., Clark, C.M., et al. (2006). Ubiquitinated TDP-43 in frontotemporal lobar degeneration and amyotrophic lateral sclerosis. Science 314, 130-133.

Phukan, J., Elamin, M., Bede, P., Jordan, N., Gallagher, L., Byrne, S., Lynch, C., Pender, N., and Hardiman, O. (2012). The syndrome of cognitive impairment in amyotrophic lateral sclerosis: a population-based study. J. Neurol. Neurosurg. Psychiatry 83, 102-108.

Pikkarainen, M., Hartikainen, P., and Alafuzoff, I. (2008). Neuropathologic features of frontotemporal lobar degeneration with ubiquitin-positive inclusions visualized with ubiquitin-binding protein p62 immunohistochemistry. J. Neuropathol. Exp. Neurol. 67, 280-298.

Pikkarainen, M., Hartikainen, P., and Alafuzoff, I. (2010). Ubiquitinated p62-positive, TDP-43-negative inclusions in cerebellum in frontotemporal lobar degeneration with TAR DNA binding protein 43. Neuropathology 30,

Renoux, A.J., and Todd, P.K. (2012). Neurodegeneration the RNA way. Prog. Neurobiol. 97, 173-189.

Renton, A.E., Majounie, E., Waite, A., Simón-Sánchez, J., Rollinson, S., Gibbs, J.R., Schymick, J.C., Laaksovirta, H., van Swieten, J.C., Myllykangas, L., et al.; ITALSGEN Consortium. (2011). A hexanucleotide repeat expansion in C9ORF72 is the cause of chromosome 9p21-linked ALS-FTD. Neuron 72, 257-268

van Blitterswijk, M., DeJesus-Hernandez, M., and Rademakers, R. (2012). How do C9ORF72 repeat expansions cause amyotrophic lateral sclerosis and frontotemporal dementia: can we learn from other noncoding repeat expansion disorders? Curr. Opin. Neurol. 25, 689-700.

Van Langenhove, T., van der Zee, J., and Van Broeckhoven, C. (2012). The molecular basis of the frontotemporal lobar degeneration-amyotrophic lateral sclerosis spectrum. Ann. Med. 44, 817-828.

Zhang, D., Iyer, L.M., He, F., and Aravind, L. (2012). Discovery of novel DENN proteins: Implications for the evolution of eukaryotic intracellular membrane structures and human disease. Front. Genet. 3, 283.

Zu, T., Gibbens, B., Doty, N.S., Gomes-Pereira, M., Huguet, A., Stone, M.D., Margolis, J., Peterson, M., Markowski, T.W., Ingram, M.A., et al. (2011). Non-ATG-initiated translation directed by microsatellite expansions. Proc. Natl. Acad. Sci. USA 108, 260-265.